

# Yielding and impact behaviour of pp/sgf/epr ternary composites with controlled morphology

J. JANCAR

*School of Chemistry, Technical University Brno, Veslarska 230, 63711 Brno, Czech Republic*

Dependencies of the yield strength ( $\sigma_{yc}$ ), yield strain ( $\varepsilon_{yc}$ ) and Charpy notched impact strength (CNIS) of polypropylene (PP) reinforced with 30 wt% short glass fibres (SGF) and ethylene–propylene random copolymer (EPR) inclusions on EPR volume fraction ( $v_e$ ) were investigated within the interval of  $v_e$  varying from 0–0.2. Only one limiting phase morphology has been attained reproducibly using a procedure based on chemical modification of PP. Adhesion enhancement between SGF and PP and complete separation between SGF and EPR was achieved by grafting PP with 2 wt% maleic anhydride (MAH). Two regions existed on  $\sigma_{yc}$  versus  $v_e$  curves in the case of complete separation of the reinforcement and elastomer. The observed increase of  $\sigma_{yc}$  with increasing  $v_e$  within the interval  $0 < v_e < 0.05$  was attributed to the change in the mode of fracture from brittle to quasi-ductile. Such an explanation has been supported by a several fold increase in  $\varepsilon_{yc}$ . Above  $v_e = 0.05$ , a monotonic decrease of  $\sigma_{yc}$  with increasing  $v_e$  was observed corresponding well with an explanation based on a reduction of matrix effective cross-section. In this interval of  $v_e$  the concentration dependence of  $\sigma_{yc}$  was described quantitatively using existing composite models and satisfactory agreement between predictions and experimental data was obtained. The CNIS increased monotonically up to  $v_e = 0.1$  for both homo- and copolymer based composites. Above  $v_e = 0.1$ , CNIS, measured at  $-20^\circ\text{C}$  using  $6 \times 4 \times 50$  mm bars, notched accordingly ASTM D256 standard, increased for copolymer based composites while it remained constant for homopolymer based materials. Physical meaning of these data is, however, obscured by the inability to separate effects of  $v_e$  from those of specimen geometry using only a single standard impact strength data.

## 1. Introduction

Yielding behaviour and toughness of a plastic are very often decisive parameters affecting materials selection and design of the final article. Yield strength,  $\sigma_y$ , can be considered a failure stress of the primary structure of a polymeric part limiting, thus, its further service. Yield strain,  $\varepsilon_{yc}$ , can in some cases serve as an important design parameter, limiting service conditions of a plastic part under complicated loading by its largest attainable deformation. Many materials which are ductile under usual test conditions can behave in a brittle manner when subjected to impact loading, especially at high strain rates, low temperatures and in the presence of design features causing localized stress concentration [1]. This is especially crucial in automotive applications, since the service conditions of many plastic parts of an automobile are exposed to impact loadings [2, 3]. The common means of determining fracture toughness as a material property are complete fracture mechanical measurements or, if a geometry dependent fracture toughness is desired, industrial standard and non-standard tests can be performed. The latter are relatively easy to perform, however, the physical meaning of the resulting data is

unclear in many cases and the unique character of these data does not allow their utilization for design purposes. The former methods are usually laborious, however, they provide a good physical foundation for data interpretation within the interval of validity of linear elastic fracture mechanics (LEFM).

Standardized impact tests (Izod, Charpy, Gardner, etc.) are the most commonly used measures of impact strength of plastics [4–9]. It was shown previously [10, 11], that in most cases comparison of standardized notched impact strength (NIS) values for materials of different composition is not a reliable indication of the relative toughness and it is of little value as a parameter for material selection. Moreover, NIS does not provide an adequate, geometry independent description of material toughness relevant for design purposes.

PP is considered a commodity polymer since it is produced in large quantities. Recent advances in stereospecific catalysis have enriched its potential for high volume engineering applications. Low price, good processability and excellent chemical resistance are among the most valued physical properties of PP. Moderate to low stiffness, moderate yield strength and

a relatively low toughness at low temperatures or in the presence of stress raisers are its major shortcomings. It is thus necessary to enhance its elastic modulus, yield strength and resistance to cracking, in order for PP to compete successfully with more expensive polycarbonates (PC), acrylonitrile butadiene-styrene copolymers (ABS), nylons, etc., in engineering applications. Most commonly, this can be achieved by incorporating rigid fillers or elastomer inclusions, the former enhancing stiffness and the latter improving toughness at low temperatures.

It has been suggested that incorporating both rigid reinforcement and elastomer inclusion can improve stiffness, yield strength and toughness above the level attained by a neat PP, at the same time. Phase morphology, i.e., spatial arrangement of the minor phases (filler, elastomer), plays a crucial role in controlling the mechanical response of such a composite. Phase morphology depends on a dynamic equilibrium between thermodynamic and rheological forces obtained as a result of a particular mixing procedure. Ideally, two limiting morphologies can be obtained, i.e., complete separation of elastomer and filler or a complete encapsulation of the rigid inclusions in elastomer shells. Thermodynamic forces tend towards complete encapsulation having the lowest overall free energy while the rheological forces tend to separate elastomer from the rigid inclusions due to a sharp gradient of shear force in the melt near the surface of solid inclusions. It is, thus, unrealistic to "tailor" these materials if no control over their phase morphology can be exercised. Varying the thermodynamic forces by chemical modification of the components at constant mixing conditions, one can achieve a great deal of control over the resulting phase morphology. It has been shown in the case of particulate fillers that grafting of maleic anhydride (MAH) or acrylic acid (AA) onto PP or EPR the two limiting morphologies, mentioned above, can be attained reproducibly.

Short glass fibres are incorporated into PP in order to increase its stiffness. Yield strength can be enhanced when a chemically modified PP (MPP) is used as a matrix with an excellent adhesion to the glass surface. Composite toughness at low temperatures is not in this case substantially higher than that of a neat PP. Hence, using the idea proven to work in particulate composites, i.e., adding elastomer inclusions, is available. One has to keep in mind, however, that the replacement of particulate fillers with SGF greatly complicates both melt rheology and mechanical analysis of these materials. For similar reasons as in the case of particulate fillers, it is not of a practical interest to deal with the lower limiting phase morphology, i.e., complete encapsulation of short fibres by the elastomer. The single step melt mixing procedure used to prepare these composites does not allow for preparation of uniformly thin elastomer layers on SGF. Hence, the presence of thick elastomer shells on the fibres eliminates the reinforcing efficiency of SGF and, thus, negates the purpose they serve in the composite. Until a technique capable of depositing thin uniform elastomer layers on fibres is developed, the only practical system is represented by the second limiting

phase morphology, i.e., complete separation of the rigid reinforcement and elastomer inclusions. In order to gain a first insight into these problems, this study has been initiated.

In this paper we report on the effect of EPR volume fraction on the yielding and impact behaviour of MPP/SGF/EPR composites with complete separation of SGF and EPR.

## 2. Experimental procedure

Neat polypropylene homopolymer (iPP) and copolymer containing 3 mol % ethylene (cPP) were supplied by Chemopetrol (Litvinov, Czech Republic, MFR = 4 g/10 min at 210 °C, 21 N). Maleated version of iPP and cPP (MPP) were supplied by the Polymer Institute Brno (Brno, Czech Republic, MFR = 20 g/10 min at 210 °C, 21 N). Ethylene-propylene random copolymer (EPR) was supplied by Himont (Ferrara, Italy,  $M_w = 180\,000$ ,  $T_g = -56$  °C). Owens Corning chopped roving (12 mm) was used as the short glass fibre (SGF) reinforcement. The fibres were heat treated in a vacuum oven at 400 °C for 2 h in order to remove organic sizing and weakly adsorbed water. The components were compounded in a PLO 651 Brabender Plasticorder at 200 °C at 50 rpm for 10 min. The dog-bone specimens for tensile tests were cut from the compression molded sheets of compounded materials. The 6 × 4 × 50 mm bars for the standardized Charpy notched impact test were notched according to ASTM D256. The notch depth was 1/3 of the specimen thickness and the notch tip radius was 0.25 mm. CNIS was calculated by dividing the fracture energy  $U$ , corrected for the kinetic energy of the flying pieces and the equipment correction, by the ligament area, i.e.,  $[B \times (D - a)]$ , where  $a$ ,  $B$  and  $D$  is the notch length, thickness and width, respectively.

An Instron 4302 Universal Tester was used in the tensile tests at room temperature and at a strain rate of 3 min<sup>-1</sup>. Reported values are averaged from 5 specimens with a standard deviation of 10%. The impact energy measurements were performed using an instrumented impact pendulum Ceast with a 4J hammer (impact speed 3.5 ms<sup>-1</sup>) at -20 °C. Data were collected using a Hitachi memory oscilloscope and the presented values are averaged from 10 specimens with a standard deviation of 10–15%. An Amray II scanning electron microscope (SEM) was used for fractographic observations of the fracture surfaces from both tensile and impact tests.

## 3. Results and discussion

### 3.1. SEM observations

SEM micrographs of the fracture surfaces have revealed an excellent adhesion between MPP and SGF even after prolonged exposure to boiling water (Fig. 1). The SEM also provides qualitative information about the failure mechanisms. The prevailing mode of failure under tensile loading conditions was an extensive, localized plastic deformation of both the matrix bulk and the interphase layer of constrained MPP. The damage zone near the crack planes was

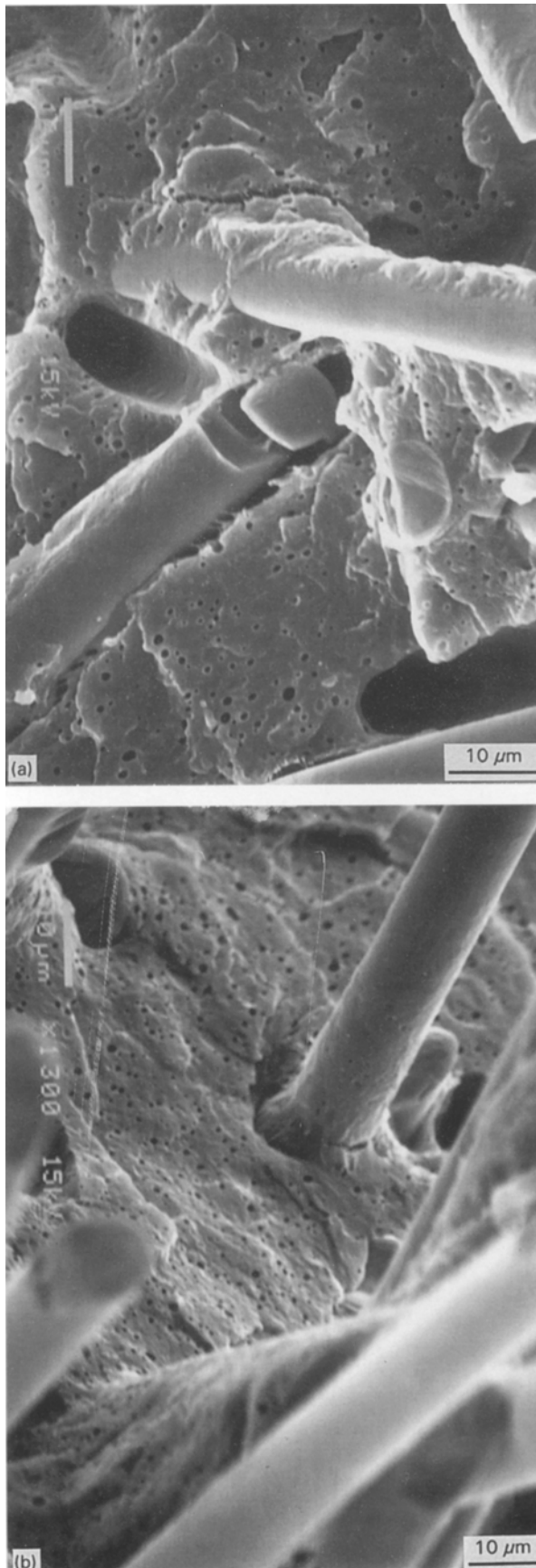


Figure 1 (a) SEM fractograph of the surface of iMPP/EPR/SGF composite with homopolymer matrix fractured at  $-20^{\circ}\text{C}$  under impact loading and (b) as in (9) but with copolymer matrix.

relatively large and extended with increasing  $v_e$ . However, a Class II character of the fracture, with brittle fracture and contained yielding, has been attained up to  $v_e = 0.10$ . In comparison to binary MPP/SGF

composites, breaking under similar conditions in a brittle manner prior to reaching the macroscopically important extent of plastic deformation, a substantially larger extent of plastic deformation near the crack planes was observed in MPP/SGF/EPR composites. This is due to the localized stress relief allowed by the presence of the EPR inclusions which reduce the yield strength of the matrix in the bulk. Above  $v_e = 0.15$ , a plastic hinging effect has been identified even in impact tests at  $-20^{\circ}\text{C}$ .

### 3.2. Yielding behaviour

A similar approach as described in currently published works [12–14] on the yielding behaviour of a rigid filler and elastomer modified PP with controlled phase morphology was utilized in order to analyse the experimental data. The SGF effect was described using the Halpin–Tsai [15] model for a yield strength of 2-d randomly oriented SGF composite:

$$\sigma_{yc}^{\text{bin}} = \eta \sigma_f v_f + \sigma_{ym}(1 - v_f), \quad (1)$$

where the maximum fibre efficiency factor  $\eta = 0.5$  can be attained for SGF with a large  $l/d$  ratio or in the case of perfect MPP/SGF adhesion,  $\sigma_{ym}$  and  $\sigma_f$  are the MPP and SGF yield strength and strength, respectively. This MPP/SGF binary composite was visualized as an “effective matrix continuum” modified with an increasing volume fraction of a uniform and random dispersion of the elastomer inclusions. As a result, the effect of elastomer inclusions on the yield strength can be quantified using a reduction of the “effective matrix” cross-section approach in the functional form proposed for example by Nicolais and Narkis [16]:

$$\sigma_{yc}^{\text{tot}} = \sigma_{yc}^{\text{bin}}(1 - 1.21v_e^{2/3}), \quad (2)$$

where  $v_e$  is the elastomer volume fraction and  $\sigma_{yc}^{\text{bin}}$  is the “effective binary matrix” yield strength expressed by Equation 1.

The solid and dashed lines in Fig. 2 represent the concentration dependence of  $\sigma_{yc}$  for the ternary composite based on maleated iPP and cPP, respectively, calculated using Equations 1 and 2. These calculated values, predicting the upper limit of attainable yield strength, have the functional form where the matrix yield strength was a multiplicative factor. Hence, the yield strength of the matrix controlled the vertical shift of the actual data along the yield strength axis, however, it did not affect the functional dependence of  $\sigma_{yc}^{\text{tot}}$  on  $v_e$ . One has to, however, keep in mind the simplifying assumptions built into the foundations of the proposed quantitative analysis. Hence, the validity of such an approach is limited to the inclusion concentrations range in which the matrix properties remain unchanged by the presence of secondary components

TABLE 1 Mechanical properties of iMPP, cMPP and SGF used in calculations

Component	$E$ [GPa]	$\sigma$ [MPa]	$\varepsilon$
iMPP	2.0	40	0.14
cMPP	1.5	26	0.19
SGF ( $l/d = 40$ )	72	1000	0.02

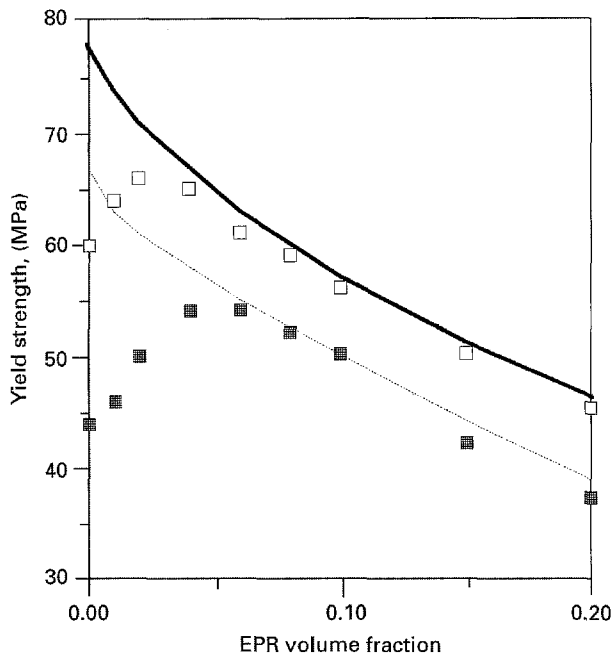


Figure 2 Dependence of the composite yield strength on EPR volume fraction at constant concentration of SGF (30 wt %) at 23 °C,  $\dot{\epsilon} = 3 \text{ min}^{-1}$ . Open squares represent iPP based composites, filled squares are for cPP based materials. Solid and dashed lines were calculated using Equations 1 and 2 for iPP and cPP composites, respectively.

and also where these components do not mechanically interact. Within these limitations, Equation 2 can be used as a first order approximation for “tailoring” composites to achieve desired yielding properties.

The discrepancy between experimental data and predictions based on Equation 2 for  $v_e < 0.05$  is caused by a change in the failure mechanism from brittle to ductile as clearly seen from the plot of yield strain  $\epsilon_{yc}$  versus  $v_e$  (Fig. 3). Since the proposed approach assumed that only a single ductile failure mode operates over the entire concentration region, one cannot expect it to work when the failure mode is a brittle one. Above  $v_e = 0.05$ , the ductile failure is restored and the agreement between predicted points and the experimental data was satisfactory. This interpretation also explains the apparently absurd increase in  $\sigma_{yc}^{\text{tot}}$  with increasing  $v_e$  at low EPR concentrations.

### 3.3. Impact behaviour

It appears from observations of fractured specimens that a change in failure mode from Class II, i.e., brittle fracture with small scale yielding, to Class III, i.e., plastic hinging, occurred above  $v_e = 0.15$ . Hence, one has been limited to a qualitative description of the experimentally determined concentrational dependence of CNIS. More importantly, however, it has not been possible to use a linear elastic fracture mechanism (LEFM) analysis of the data even below  $v_e = 0.15$  due to the fact that the effects of  $v_e$  and test geometry on the fracture energy cannot be separated based on a single standard CNIS data point. As a result, the measured concentrational dependencies of CNIS depicted in Fig. 4 are unique to the particular test geometry used in this study. It is, thus, meaning-

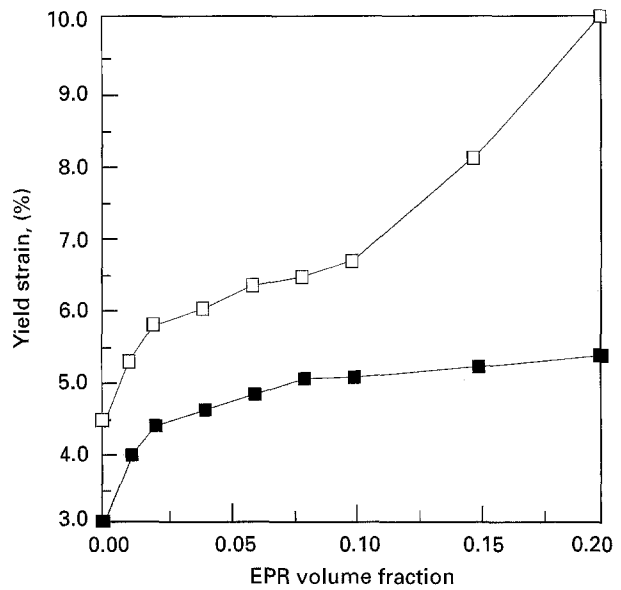


Figure 3 Compositional dependence of the yield strain under the same conditions as in Fig. 2. ■ = iPP, □ = cPP.

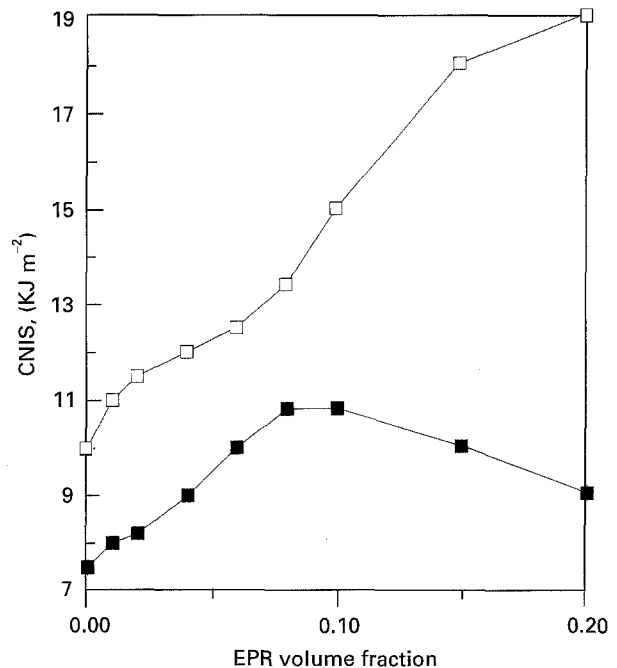


Figure 4 Dependence of the CNIS at  $-20^\circ\text{C}$  on EPR volume fraction. Symbols as in Fig. 3.

less to compare data based on the two matrices, i.e., iPP and cPP, in addition a comparison within a series of materials with different elastomer contents is useless. The questionable physical meaning of CNIS for the comparison of the relative toughness of materials of different compositions has been discussed [2].

At low  $v_e$ , when the fracture is not obscured by large plastic deformations of the matrix, standardized CNIS values showed reasonably higher toughness for the cPP based material compared to the iPP based composite at the same specimen geometry. It seems reasonable to suggest that the major contributing failure mechanism is the plastic deformation of a thin layer of matrix adhered to the fibres and fibre pull-out (Fig. 1). Increasing the EPR concentration above  $v_e = 0.1$  leads to an increase in CNIS in the case of the cPP

based composites, however, a steady decrease in impact strength was observed for the iPP based materials. These trends were unique to the test conditions described in the experimental procedure paragraph of this paper. In order to draw any physically sound conclusion regarding the compositional dependence of the fracture toughness independent of the specimen geometry, a full fracture mechanics study must be performed.

#### 4. Conclusions

Yielding behaviour and the standard Charpy notched impact strength of MPP reinforced with 30 wt % SGF and variable EPR concentration for automotive applications was investigated using tensile tests and a standardized Charpy impact test geometry. The mode of fracture was qualitatively evaluated using SEM observations. The adhesion between SGF and MPP was excellent. Large plastic deformations in the matrix, fibre pull-out and plastic deformations of the interphase in the vicinity of fibres were the primary dissipative processes accompanying both yielding and impact fracture of the composites investigated.

Predictions of  $\sigma_{yc}^{tot}$  based on existing composite models agreed satisfactorily with experimental data above  $v_e = 0.05$  due to a change of the failure mode from brittle to ductile. The matrix type did not affect the functional dependence of the  $\sigma_{yc}^{tot}$  versus  $v_e$ , however, it was the primary factor in controlling the actual value of the yield strength of the composites. Equations 1 and 2 can, thus, be considered a first approximation to "tailoring" composites for a particular end application.

It appears clear from our data that comparison of standardized CNIS for materials of different composition is not a reliable indication of the relative material

toughness. CNIS has thus little value in materials selection for design purposes since it does not allow separation of the effects of structural variables from those of test geometry.

#### Acknowledgement

The author thanks Professor A. T. DiBenedetto for helpful discussions and interest in this work.

#### References

1. C. B. BUCKNALL, "Toughened Plastics" (Applied Science, London 1977).
2. S. K. GAGGAR, "Instrumented Impact Testing of Plastics and Composite Materials", edited by S. L. Kessler, G. C. Adams, S. B. Driscoll and D. R. Ireland (ASTM 6, Baltimore 1987) p. 236.
3. N. S. KAKARALA, J. L. ROCHE, *ibid* p. 144.
4. ASTM D256-84 Standard.
5. ISO 179 Standard, ISO 180 Standard.
6. DIN 53 373 Standard (German Standards Institute).
7. J. G. WILLIAMS, "Fracture Mechanics of Polymers", (Ellis Horwood, Chichester, UK, 1987) p. 270.
8. J. KREITER and R. KNODEL, *Kunststoffe* **83** (1993) 889.
9. J. JANCAR, A. DIANSELMO, A. T. DIBENEDETTO and J. KUCERA, *Polymer* **34** (1993) 1684.
10. J. JANCAR and A. T. DIBENEDETTO, in Proceedings of the Annual Technical Conference of the Society of Plastic Engineers (SPE), May, 1994 (SPE, Brockfield USA, 1994) vol. II, p. 1710.
11. *Idem.*, *Polym. Eng. Sci.* **34** (1994) 1799.
12. *Idem.*, *Sci. Engng Compos. Mater.* **3** (1994) 217.
13. *Idem.*, *J. Mater. Sci.* **30** (1995) 1601.
14. *Idem.*, *ibid* **30** (1995) 2438.
15. B. D. AGARWAL and L. J. BROUTMAN, "Analysis and Performance of Fibre Composites", (J. Wiley, New York, 1980) ch. 3, p. 71.
16. L. NICOLAIS and M. NARKIS, *Polym. Eng. Sci.* **11** (1971) 194.

Received 10 August

and accepted 21 December 1995